Research Article

Jia Shao, Kai Deng, Le Chen, Chaomeng Guo, Congshan Zhao, Jiayuan Cui, Tongan Shen, Kewei Li, Jianqiao Liu*, and Ce Fu*

Aqueous synthesis of Nb-modified SnO_2 quantum dots for efficient photocatalytic degradation of polyethylene for *in situ* agricultural waste treatment

https://doi.org/10.1515/gps-2021-0046
received April 15, 2021; accepted July 09, 2021

Abstract: Low density polyethylene is widely used in agricultural production. It is of low cost and able to significantly improve the quality of fruits. However, its decomposition under natural circumstances needs more than one hundred of years. If not removed in time, it is hazardous to the ecological environment and crops. Up to now, the removal techniques of polyethylene films are polluted, expensive, and difficult to employ. A novel method is proposed for *in situ* removal of polyethylene by an effective and environmental friendly technique with low cost. The Nb-modified SnO_2 quantum dots are prepared for the efficient photocatalytic degradation of polyethylene under visible light. The green synthesis of the photocatalyst includes the procedures of hydrolysis, oxidation, and hydrothermal treatment in aqueous solution. The Nb-modified SnO_2 has a band gap of 2.95 eV, which enhances its absorption of visible light. A degradation efficiency of 29% is obtained within 6 h under visible irradiation. The hydroxyl radicals ($^{\bullet}OH$) are main active species in the degradation process. The prepared Nb-SnO_2 quantum dots demonstrate a promising application in the photocatalytic degradation of polyethylene, contributing a novel strategy for the *in situ* treatment of agricultural wastes.

Keywords: Nb-modified SnO_2, visible-light photocatalysis, polyethylene, quantum dot, environment remediation

1 Introduction

Low density polyethylene films are widely used in agricultural production because they are able to improve the fruit quality by collecting solar irradiation and enhancing photosynthesis. Millions of tons of polyethylene products are fabricated annually due to the increasing market demands [1,2]. However, these polyethylene products are hazardous to ecological environment and worthless to recycle because they are difficult to be degraded in natural circumstances, fragile after long-term usage, and valueless to be reused [3]. Thus, a great amount of polyethylene wastes are deposited in rural environment and lead to heavy plastic pollution after accumulation [4,5]. Moreover, some polyethylene products contain metallic film on top so that they are highly conductive. High voltage wires for energy transmission and high-speed railway trains are in risks if conductive polyethylene films are not under control. The potential risks from power failure include collisions between high-speed trains and disturbance of power supply to cities/factories, causing a great direct or indirect economic loss. Three methods are usually used to remove polyethylene products, such as mechanical recycling, incineration, and burying [3]. Nevertheless, they suffer from the drawbacks of high cost and environmental pollution. Thus, a novel method is expected for the removal of polyethylene products by a technique with high efficiency, low cost, simple operation, and environmental friendship.

* **Corresponding author: Jianqiao Liu,** College of Information Science and Technology, Dalian Maritime University, Dalian 116026, Liaoning, China, e-mail: jqliu@dlmu.edu.cn
* **Corresponding author: Ce Fu,** College of Information Science and Technology, Dalian Maritime University, Dalian 116026, Liaoning, China, e-mail: fu_ce@dlmu.edu.cn
Jia Shao, Kai Deng, Le Chen: College of Environmental Science and Engineering, Dalian Maritime University, Dalian 116026, Liaoning, China
Chaomeng Guo, Jiayuan Cui, Tongan Shen, Kewei Li: College of Information Science and Technology, Dalian Maritime University, Dalian 116026, Liaoning, China
Congshan Zhao: College of Transportation Engineering, Dalian Maritime University, Dalian 116026, Liaoning, China

Photocatalysis is an emerging advanced technique in recent decades. The photocatalysts, usually based on functional semiconductors, absorb external irradiation and accelerate redox reactions by releasing reactive species excited from photogenerated electron-hole pairs. Thus, they are used in the applications of water splitting for hydrogen [6,7], organic degradation [8–11], heavy metal ion reduction [12,13], and anti-bacteria [14,15]. As the environmental issues are serious concern nowadays, the photocatalytic organic removal receives attention from a variety of fields. As a sustainable approach for environmental remediation, photocatalysis is able to remove plethora of recalcitrant pollutants [16–18] and is proved to be a smart alternative to mitigate environmental problems as it may complete rapid conversion from organic compounds to green products [19,20]. However, the mass application of emerging photocatalysis is still facing the challenges, such as the potential risks to human or ecological health as well as the uncertainties associated with dispersal, excotoxicity, persistency, bioaccumulation, and reversibility of photocatalysts [21]. Nevertheless, the photocatalytic activities are promising as they can make utilization of solar energy with low cost and green process. Thus, the design and synthesis of photocatalysts have become a hot topic at present [22–28]. Among nanostructured photocatalysts, the tin oxide (SnO_2) quantum dot (QD) is attractive because it is stable, inexpensive, nontoxicity, and easy to prepare [29–31]. Its strong positive valence band not only prevents self-decomposition under long-time irradiation, but also benefits the generation of hydroxyl radicals, which are able to break the benzene ring for the decomposition of volatile organic compounds [32,33]. However, the stoichiometric SnO_2 bulk is wide band gap semiconductor. The band gap of 3.6 eV [34] inhibits its photocatalytic application because it absorbs little visible light, which composes the main part of the solar irradiation spectrum. Thus, modifications should be made to reduce the band gap of SnO_2-based materials for improving the absorption of visible light during photocatalytic activities. The incorporation of transition metal elements is one of the routes [35].

In the present work, Nb-modified SnO_2 QDs are synthesized via an aqueous-based method. The morphology, composition, and optical characteristics are investigated. The Nb-SnO_2 QDs are employed to degrade polyethylene and the photocatalytic properties are discussed based on the performances at various QD concentrations and irradiation sources. The main active species in the photocatalytic activities and the degradation mechanism are discussed.

2 Materials and methods

The aqueous synthesis of SnO_2 QDs was completed by using a one-step method [36,37]. Stannous chloride of 2.257 g and thiourea of 0.077 g were commingled into deionized water of 50 mL. The mixture was stirred in a magnetic stirring apparatus at room temperature for 24 h. Then, the solution of SnO_2 QDs was obtained. Niobium ammonium oxalate of 0.0425 g was added into the SnO_2 QD solution of 10 mL and the Nb-added solution was put into a teflon autoclave for hydrothermal treatment at 160°C for 6 h. After cooling to room temperature, the Nb-modified SnO_2 QDs for photocatalysts were obtained.

The X-ray diffraction (XRD, D/MAX-Ultima, Rigaku, Tokyo, Japan) was used to determine the crystal structure, crystallite size, and lattice parameters of the Nb-modified SnO_2 QDs. The chemical composition and bonding details were confirmed by X-ray photoelectron spectroscopy (XPS, Thermo Scientific ESCALAB 250 XI, ThermoFisher Scientific, Waltham, MA, USA). The surface morphology and lattice fringes were observed by the high resolution transmission electron microscopy (HRTEM, JEM-3200FS, JEOL, Tokyo, Japan). The ultraviolet-visible spectroscopy (UV-Vis) was used to collect and determine the absorption spectrum and band gap (E_g).

The artificial irradiation sources of 50 and 300 W were used to examine the photocatalytic properties. The polyethylene film products were mechanically crashed and commingled with the Nb-SnO_2 QD solution. During the photocatalytic activities, the mixture was stirring at room temperature. The degradation efficiency (η) of the photocatalytic process was defined as:

$$\eta = (m_1 - m_2)/m_1 \times 100\% \quad (1)$$

where m_1 and m_2 were the initial weight and final weight of polyethylene film before and after photocatalytic activity.

The trapping experiments of possible active radicals in the degradation process were carried out by introducing the radical scavengers of isopropanol (IPA), potassium bromate ($KBrO_3$), and ammonium oxalate [$(NH_4)_2C_2O_4$]. Each radical scavenger of 2 mmol/L was added before the irradiation.

3 Results and discussion

3.1 Morphology and composition

As shown in Figure 1a, four main peaks in the XRD pattern at 26.5°, 33.9°, 38.2°, and 51.7° are observed,

corresponding to the planes of (110), (101), (200), and (211). The pattern is in agreement with the standard pattern [38]. A slight enlargement in crystal lattice caused by Nb modification is concluded by the lattice parameters of $a(b) = 4.7429$ Å and $c = 3.1966$ Å. No Nb-containing phase is detected so that the Nb atoms are incorporated into the SnO_2 QD lattice. According to the Scherrer's formula, the average crystallite size is calculated to be 5.3 nm. The morphology of Nb-modified SnO_2 QDs is shown in Figure 1b. The average grain size is found to be 5.6 nm, which is close to the result from XRD analysis. The characteristic plane distances of 0.321–0.325 nm are found and they are associated with the (110) plane of SnO_2 crystal lattice. Figure 1c shows the XPS survey spectrum after calibration [39]. The Nb peak is observed at 207.63 eV, demonstrating the successful incorporation of Nb atoms into the SnO_2 lattice. The XPS spectrum of O 1s is shown in Figure 1d, in which an asymmetric peak is observed. It is deconvoluted with sub-peaks obtained at 531.76 and 530.97 eV. They are ascribed to different chemical states of oxygen in the lattice. The former one centered at 531.76 eV is resulted from the stoichiometric lattice of SnO_2. The other one centered at 530.97 eV is caused by the oxygen vacancies, which are inherent in SnO_2 grains. Compared to pristine SnO_2 QDs [40], the Nb modification leads to red shifts to both sub-peaks of O 1s and it may benefit the stability of oxygen-deficient SnO_2 QDs.

3.2 Optical characterization

The UV-Vis absorption of the Nb-SnO_2 QDs is plotted in Figure 2a. After being converted to the Tauc relation [41] in Figure 2b, the E_g is calculated to be 2.95 eV, which is located in the region of visible light in the solar light spectrum. Therefore, it is possible for the Nb-modified SnO_2 QDs to be efficient photocatalyst under visible light. Figure 2c reveals the XPS valence band spectrum of Nb-modified SnO_2 QDs. The top edge position of valence band (E_V) is 3.58 eV. Thus, the bottom edge position of conduction band (E_C) is 0.63 eV according to $E_C = E_V - E_g$.

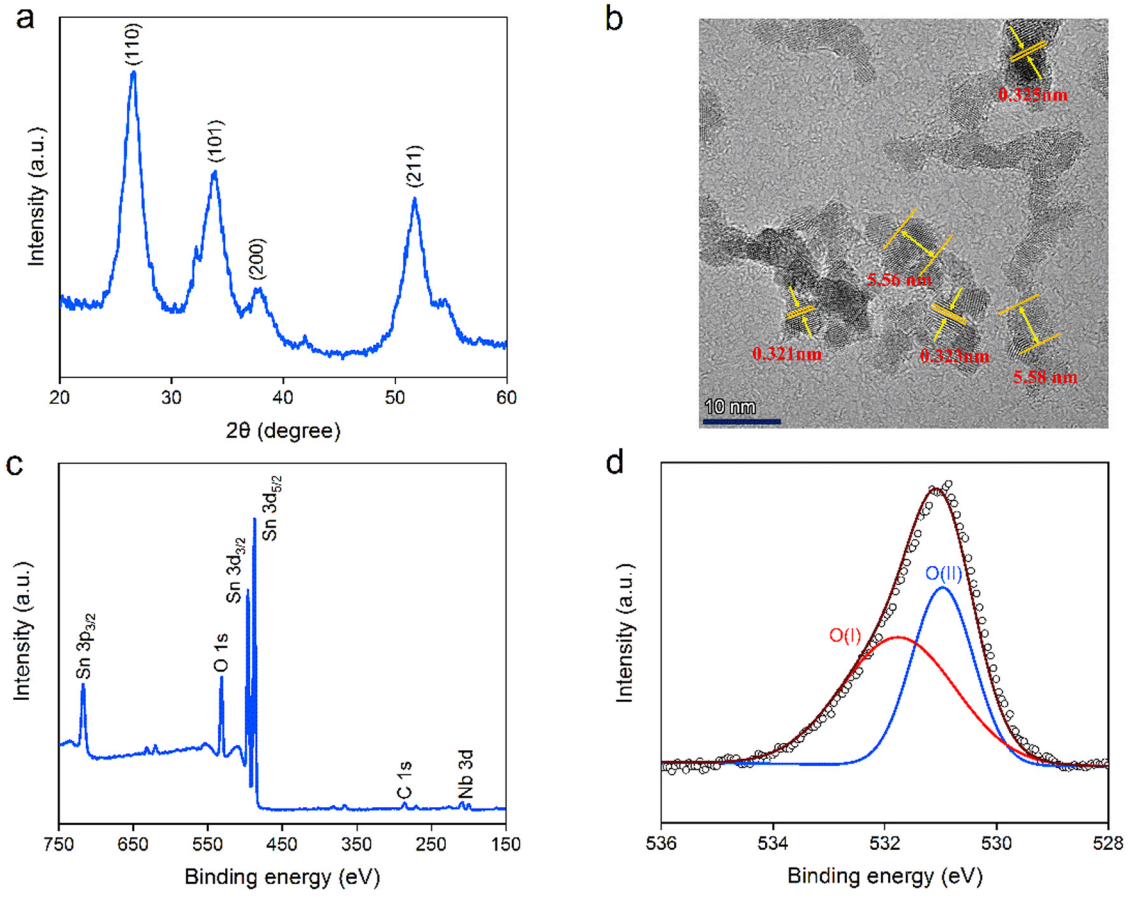

Figure 1: Composition and morphology of Nb-modified SnO_2 quantum dots: (a) XRD pattern, (b) HRTEM, (c) XPS survey spectrum, and (d) XPS O 1s spectrum.

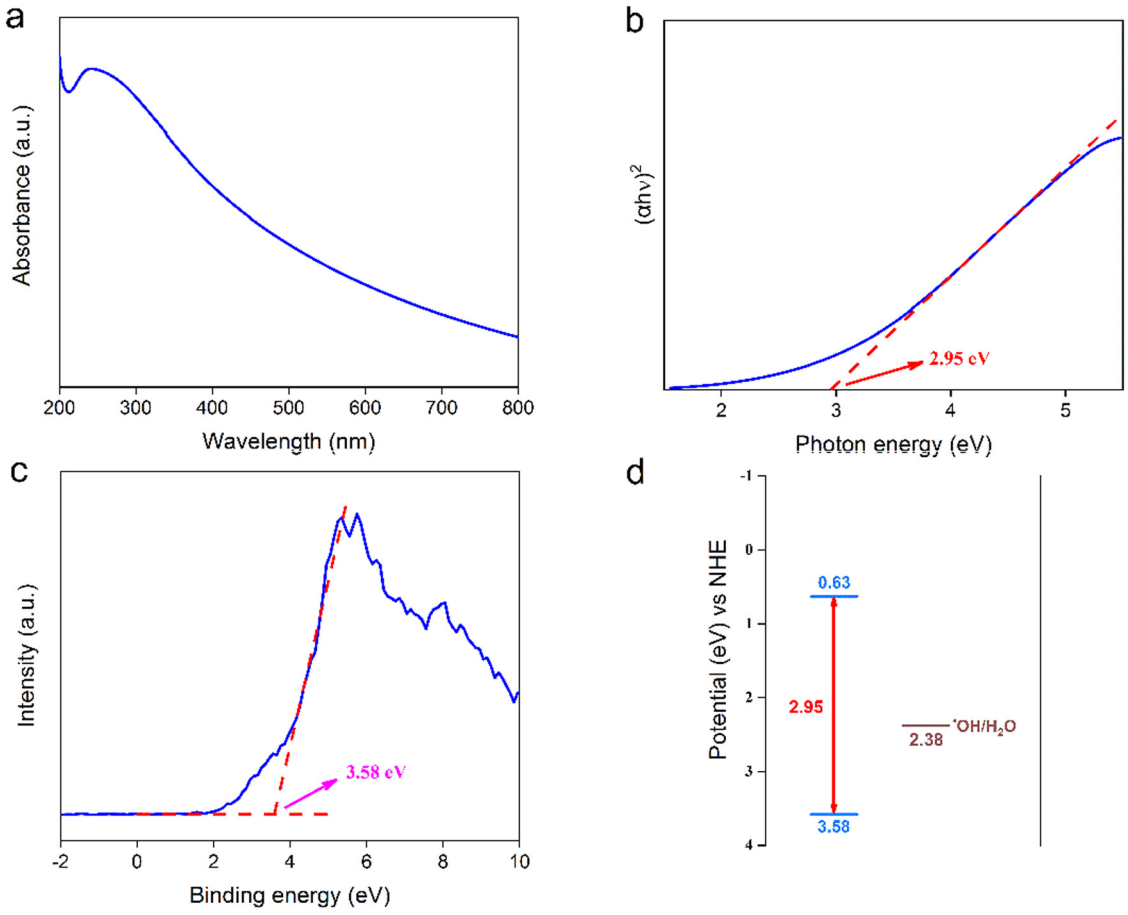

Figure 2: Optical properties of Nb-modified SnO_2 quantum dots: (a) UV-Vis absorption spectrum, (b) Tauc plot for band gap evaluation, (c) valence band spectrum, and (d) band structure.

Hence, the band structure of QD photocatalysts is displayed in Figure 2d. It is found that E_V is greater than the redox potential of aqueous solution so that the photogenerated holes could combine with H_2O to produce hydroxyl radicals ($^{\bullet}OH$) with strong ability of oxidation. Thus, the present Nb-modified SnO_2 QDs have proficient photocatalytic abilities in the degradation of polyethylene.

3.3 Polyethylene degradation

Figure 3a plots the 3-hour photocatalytic degradation efficiency of polyethylene at various concentrations of Nb-modified SnO_2 QDs under 300 W irradiation. The concentration of Sn atoms in the aqueous solution is used to indicate the concentration of QDs. The maximum photocatalytic degradation of 17% is observed at QD concentration of 5×10^{-4} mol/L, which is considered as the optimized concentration for photocatalytic degradation. Figure 3b illustrates the time-dependent photocatalytic degradation of polyethylene at the optimum concentration of 5×10^{-4} mol/L. The degradation efficiency increases to 29% within 6 h and the linear fitting indicates a degradation rate of 4.6%/h.

The radical scavengers of IPA, $KBrO_3$, and $(NH_4)_2C_2O_4$ are used to determine the existence of active radicals of $^{\bullet}OH$, e^-, and h^+, which can be captured by the scavengers. The degradation performances are significantly reduced by IPA, $KBrO_3$, and $(NH_4)_2C_2O_4$ to 4.0%, 6.1%, and 4.6%, respectively, as shown in Figure 3c. Therefore, all of $^{\bullet}OH$, e^-, and h^+ are confirmed to be the active radicals in the degradation process, when $^{\bullet}OH$ makes the greatest contribution in the photocatalytic activities.

The effect of irradiation sources on the photocatalytic degradation efficiency is revealed in Figure 3d. The Nb-modified SnO_2 QDs show better photocatalytic performances under ultraviolet light, which has higher photon energy to complete electron transition from the top edge position of valence band to the bottom edge position of conduction band. As ultraviolet irradiation is also a part

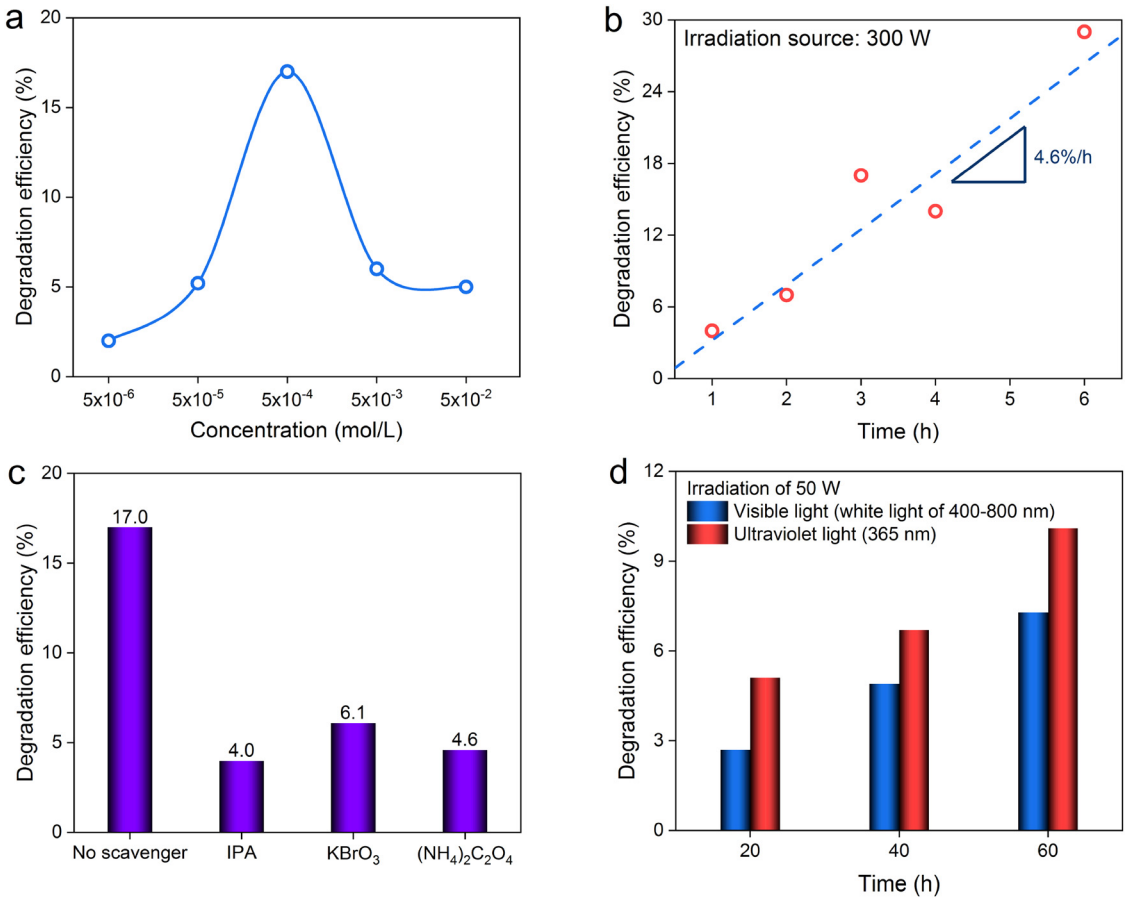

Figure 3: Photocatalytic properties of Nb-modified SnO_2 quantum dots in polyethylene degradation: (a) effect of QD concentration, (b) time-dependent photocatalytic performance, (c) trapping experiments of active radicals, and (d) effect of irradiation source.

of solar energy, its utilization could benefit the photocatalytic degradation of polyethylene for *in situ* agriculture waste treatment.

The present Nb-modified SnO_2 QDs demonstrate an efficient photocatalytic property in the degradation of polyethylene for *in situ* agriculture waste treatment. It is known that the band gap of stoichiometric SnO_2 bulk is 3.6 eV. The quantum confinement effect elevates the band gap to over 4 eV in ultrasmall QD system [42]. These values of the band gap lead to difficulties for the SnO_2 nanomaterial in photocatalytic applications. Table 1 illustrates the properties of the SnO_2 QDs before and after Nb modifications. Compared to the pristine SnO_2 QDs [40], Nb modification reduces the band gap to 2.95 eV, which is in the range of visible light. The incorporation of Nb in the SnO_2 lattice introduces energy levels of defects [43], leading to shifts of E_V and E_C positions. The 4d orbit electrons of transition metals, such as Nb, may occupy the lower energy levels near the bottom of E_C, which is consequently extended to the Fermi level. These electrons in the 4d orbit are able to transit from the occupied states to the unoccupied states in the conduction band. Therefore, the photocatalytic properties are enhanced by the incorporation of transition metal Nb [35]. Meanwhile, the E_V of the present photocatalyst at 3.58 eV is above the redox potential for the formation of highly oxidative hydroxyl radicals ($^{\bullet}OH$), which are the

Table 1: Comparison of SnO_2 QD properties before and after Nb modification

	Pristine SnO_2	Nb-doped SnO_2
Reference	[40]	This work
Lattice parameter of $a(b)$ (Å)	4.7710	4.7429
Lattice parameter of c (Å)	3.1950	3.1966
Grain size (nm)	2.0	5.3
E_g (eV)	4.20	2.95
E_C (eV)	−0.55	0.63
E_V (eV)	3.65	3.58
Photocatalytic active radicals	h^+ and $O_2^{-\bullet}$	$^{\bullet}OH$, e^-, and h^+

Table 2: Photocatalytic properties in polyethylene degradation of Nb-modified SnO_2 QDs compared with other typical semiconductor photocatalysts

Photocatalyst	Irradiation source	Reaction time	Efficiency (%)	Reference
TiO_2@AlH	1,800 W ultraviolet light	72 h	20	[44]
C/N-TiO_2	50 W visible light	50 h	71	[45]
$NiAl_2O_4$	350 W visible light	5 h	12.5	[46]
Fe-ZnO	Sunlight	120 h	41.3	[47]
N-TiO_2	27 W visible light	20 min	6.4	[48]
NiO	Sunlight	240 h	33	[49]
PPy/TiO_2	Sunlight	240 h	35.4	[50]
TiO_2 nanotubes	85 W visible light	45 days	43	[51]
PAM-TiO_2	40 W ultraviolet light	520 h	39.85	[52]
Nb-SnO_2 QDs	300 W visible light	6 h	29	This work

resultants of water and photogenerated holes. Therefore, the present Nb-modified SnO_2 QDs are able to be used as efficient photocatalysts for the *in situ* degradation of polyethylene. Compared with other typical semiconductor photocatalysts [44–52], the present Nb-SnO_2 QDs demonstrate excellent performances in polyethylene degradation, as shown in Table 2.

The molecule degradation mechanism [45,53] could be described by the following Eqs. 2–6:

$$(-CH_2-\dot{C}H-)_n + {}^{\bullet}OH \rightarrow (-CH_2-\dot{C}H-)_n + H_2O \quad (2)$$

$$(-CH_2-\dot{C}H-)_n + O_2 \rightarrow (-CH_2-{}^{\bullet}OOCH-CH_2-)_n \quad (3)$$

$$(-CH_2-CH_2-)_n + (-CH_2-{}^{\bullet}OOCH-CH_2-)_n \rightarrow (-CH_2-HOOCH-CH_2-)_n + (-CH_2-\dot{C}H-)_n \quad (4)$$

$$(-CH_2-HOOCH-CH_2-)_n \rightarrow (-CH_2-{}^{\bullet}OCH-CH_2-)_n + {}^{\bullet}OH \quad (5)$$

$$(-CH_2-{}^{\bullet}OCH-CH_2-)_n + (-CH_2-CH_2-)_n \rightarrow (-CH_2-\dot{C}H-)_n + (-CH_2-HOCH-CH_2-)_n \quad (6)$$

The Eq. 2 indicates that the photocatalytic-generated $^{\bullet}OH$ radicals interact with polyethylene, resulting in polyethylene alkyl radicals, which are converted into peroxy radicals after oxidation, as Eq. 3. Then, as Eq. 4, the peroxy radicals extract H atoms from polyethylene with hydroperoxide obtained. It cleaves the weak O–O bonds by producing highly active radicals of oxy and $^{\bullet}OH$, as Eq. 5. The resultants then extract hydrogen from the polyethylene chains, as Eq. 6, and thus the photocatalytic degradation of polyethylene is accomplished. The mechanism above demonstrates that no chemicals except for photocatalysts are needed in the photocatalytic process and solar energy is of good utilization, exhibiting the advantages of photocatalytic degradation technique.

4 Conclusion

Nb-modified SnO_2 QDs are synthesized by an aqueous route for the photocatalytic degradation of polyethylene, which is widely used but difficult to recycle and hazardous to ecological environment. The green synthesis of Nb-modified SnO_2 QDs is completed by procedures of hydrolysis, oxidation, and hydrothermal treatment. The prepared QDs demonstrate efficient photocatalytic performances for the removal of polyethylene. At the optimum QD concentration of 5×10^{-4} mol/L, the degradation efficiency reaches 29% within 6 h. The proficient photocatalytic properties are ascribed to the band structure, which is modified by Nb incorporation. The band gap is 2.95 eV and the position of valence band top is 3.58 eV, which is above the oxidation potential of water. The highly oxidative hydroxyl radicals ($^{\bullet}OH$), resulting from water and photogenerated holes, are the main active species in the photocatalytic degradation of polyethylene. The present work develops the nontoxic SnO_2 QD photocatalysts and provides a novel strategy for the *in situ* removal of polyethylene from agricultural wastes.

Funding information: This work is financially supported by the Agricultural Science and Technology Innovation Program of Chinese Academy of Agricultural Sciences (Grant No. CAAS-ZDRW202110) and Fundamental Research Funds for the Central Universities (Grant No. 3132019348).

Author contributions: Jia Shao: methodology, writing – original draft; Kai Deng: methodology, data analysis; Le Chen: experiments, writing – original draft; Chaomeng Guo: experiments; Congshan Zhao: experiments; Jiayuan Cui: experiments; Tongan Shen: experiments; Kewei Li:

experiments; Jianqiao Liu: writing – editing and review, project administration; Ce Fu: project administration.

Conflict of interest: Authors state no conflict of interest.

References

[1] Li K, Ma D, Wu J, Chai C, Shi Y. Distribution of phthalate esters in agricultural soil with plastic film mulching in Shandong Peninsula, East China. Chemosphere. 2016;164:314–21. doi: 10.1016/j.chemosphere.2016.08.068.

[2] Wang T, Yu C, Chu Q, Wang F, Lan T, Wang J. Adsorption behavior and mechanism of five pesticides on microplastics from agricultural polyethylene films. Chemosphere. 2020;244:125491. doi: 10.1016/j.chemosphere.2019.125491.

[3] Ren X. Biodegradable plastics: a solution or a challenge? J Clean Prod. 2003;11(1):27–40. doi: 10.1016/S0959-6526(02)00020-3.

[4] Hou L, Xi J, Chen X, Li X, Ma W, Lu J, et al. Biodegradability and ecological impacts of polyethylene-based mulching film at agricultural environment. J Hazard Mater. 2019;378:120774. doi: 10.1016/j.jhazmat.2019.120774.

[5] Muñoz K, Buchmann C, Meyer M, Schmidt-Heydt M, Steinmetz Z, Diehl D, et al. Physicochemical and microbial soil quality indicators as affected by the agricultural management system in strawberry cultivation using straw or black polyethylene mulching. Appl Soil Ecol. 2017;113:36–44. doi: 10.1016/j.apsoil.2017.01.014.

[6] Xie M, Zhang Z, Han W, Cheng X, Li X, Xie E. Efficient hydrogen evolution under visible light irradiation over $BiVO_4$ quantum dot decorated screw-like SnO_2 nanostructures. J Mater Chem A. 2017;5(21):10338–46. doi: 10.1039/C7TA01415E.

[7] Tian B, Tian B, Smith BB, Scott MC, Lei Q, Hua R, et al. Facile bottom-up synthesis of partially oxidized black phosphorus nanosheets as metal-free photocatalyst for hydrogen evolution. PNAS. 2018;115(17):4345–50. doi: 10.1073/pnas.1800069115.

[8] Bhembe YA, Lukhele LP, Hlekelele L, Ray SS, Sharma A, Vo D-VN, et al. Photocatalytic degradation of nevirapine with a heterostructure of few-layer black phosphorus coupled with niobium (V) oxide nanoflowers (FL-BP@Nb_2O_5). Chemosphere. 2020;261:128159. doi: 10.1016/j.chemosphere.2020.128159.

[9] Moreno YP, da Silva WL, Stedile FC, Radtke C, dos Santos JHZ. Micro and nanodomains on structured silica/titania photocatalysts surface evaluated in RhB degradation: effect of structural properties on catalytic efficiency. Appl Surf Sci Adv. 2021;3:100055. doi: 10.1016/j.apsadv.2021.100055.

[10] Ren Q, Wei F, Chen H, Chen D, Ding B. Preparation of Zn-MOFs by microwave-assisted ball milling for removal of tetracycline hydrochloride and Congo red from wastewater. Green Process Synth. 2021;10(1):125–33. doi: 10.1515/gps-2021-0020.

[11] Manalu SP, Natarajan TS, Guzman MD, Wang Y-F, Chang T-C, Yen F-C, et al. Synthesis of ternary g-C_3N_4/Bi_2MoO_6/TiO_2 nanotube composite photocatalysts for the decolorization of dyes under visible light and direct sunlight irradiation. Green Process Synth. 2018;7(6):493–505. doi: 10.1515/gps-2017-0077.

[12] Zhang L, Niu C-G, Liang C, Wen X-J, Huang D-W, Guo H, et al. One-step in situ synthesis of CdS/SnO_2 heterostructure with excellent photocatalytic performance for Cr(VI) reduction and tetracycline degradation. Chem Eng J. 2018;352:863–75. doi: 10.1016/j.cej.2018.07.102.

[13] Wan Z, Zhang G, Wu X, Yin S. Novel visible-light-driven Z-scheme $Bi_{12}GeO_{20}$/g-C_3N_4 photocatalyst: oxygen-induced pathway of organic pollutants degradation and proton assisted electron transfer mechanism of Cr(VI) reduction. Appl Catal B. 2017;207:17–26. doi: 10.1016/j.apcatb.2017.02.014.

[14] Siddiqui H, Qureshi MS, Haque FZ. Biosynthesis of flower-shaped CuO nanostructures and their photocatalytic and antibacterial activities. Nano-Micro Letter. 2020;12(1):29. doi: 10.1007/s40820-019-0357-y.

[15] He D, Zhang Z, Xing Y, Zhou Y, Yang H, Liu H, et al. Black phosphorus/graphitic carbon nitride: A metal-free photocatalyst for "green" photocatalytic bacterial inactivation under visible light. Chem Eng J. 2020;384:123258. doi: 10.1016/j.cej.2019.123258.

[16] Khan MM, Adil SF, Al-Mayouf A. Metal oxides as photocatalysts. J Saudi Chem Soc. 2015;19(5):462–4. doi: 10.1016/j.jscs.2015.04.003.

[17] Liu Y, Zeng X, Hu X, Hu J, Zhang X. Two-dimensional nanomaterials for photocatalytic water disinfection: recent progress and future challenges. J Chem Technol Biotechnol. 2019;94(1):22–37. doi: 10.1002/jctb.5779.

[18] Zhang X, Liu Y. Nanomaterials for radioactive wastewater decontamination. Environ Sci Nano. 2020;7(4):1008–40. doi: 10.1039/C9EN01341E.

[19] Jiang L, Wang Y, Feng C. Application of photocatalytic technology in environmental safety. Proc Eng. 2012;45:993–7. doi: 10.1016/j.proeng.2012.08.271.

[20] Regmi C, Dhakal D, Lee SW. Visible-light-induced Ag/BiVO4 semiconductor with enhanced photocatalytic and antibacterial performance. Nanotechnology. 2018;29(6):064001. doi: 10.1088/1361-6528/aaa052.

[21] Ganie AS, Bano S, Khan N, Sultana S, Rehman Z, Rahman MM, et al. Nanoremediation technologies for sustainable remediation of contaminated environments: recent advances and challenges. Chemosphere. 2021;275:130065. doi: 10.1016/j.chemosphere.2021.130065.

[22] Wang Y, Wu J, Yan Y, Li L, Lu P, Guan J, et al. Black phosphorus-based semiconductor multi-heterojunction TiO_2-$BiVO_4$-BP/RP film with an in situ junction and Z-scheme system for enhanced photoelectrocatalytic activity. Chem Eng J. 2021;403:126313. doi: 10.1016/j.cej.2020.126313.

[23] Song T, Hou L, Long B, Ali A, Deng G-J. Ultrathin MXene "bridge" to accelerate charge transfer in ultrathin metal-free 0D/2D black phosphorus/g-C_3N_4 heterojunction toward photocatalytic hydrogen production. J Colloid Interface Sci. 2021;584:474–83. doi: 10.1016/j.jcis.2020.09.103.

[24] Zhao Y, Wang J, Huang H, Cong T, Yang S, Chen H, et al. Growth of carbon nanocoils by porous α-Fe_2O_3/SnO_2 catalyst and its buckypaper for high efficient adsorption. Nano-Micro Letter. 2020;12(1):23. doi: 10.1007/s40820-019-0365-y.

[25] Zeng T, Shi D, Cheng Q, Liao G, Zhou H, Pan Z. Construction of novel phosphonate-based MOF/P–TiO_2 heterojunction photocatalysts: Enhanced photocatalytic performance and mechanistic insight. Environ Sci Nano. 2020;7(3):861–79. doi: 10.1039/C9EN01180C.

[26] Zhang Y, Liu C, Pang G, Jiao S, Zhu S, Wang D, et al. Hydrothermal synthesis of a $CaNb_2O_6$ hierarchical micro/nanostructure and its enhanced photocatalytic activity. Eur J Inorg Chem. 2010;2010(8):1275–82. doi: 10.1002/ejic.200900853.
[27] Wang W, Zhang J, Liang D, Li Y, Xie Y, Wang Y, et al. Anodic oxidation growth of lanthanum/manganese-doped TiO_2 nanotube arrays for photocatalytic degradation of various organic dyes. J Mater Sci Mater Electron. 2020;31(11):8844–51. doi: 10.1007/s10854-020-03419-2.
[28] El-Shafey AM. Carbon dots: discovery, structure, fluorescent properties, and applications. Green Process Synth. 2021;10(1):134–56. doi: 10.1515/gps-2021-0006.
[29] Liu J, Lv J, Shi J, Wu L, Su N, Fu C, et al. Size effects of tin oxide quantum dot gas sensors: From partial depletion to volume depletion. J Mater Res Technol. 2020;9(6):16399–409. doi: 10.1016/j.jmrt.2020.11.107.
[30] Liu J, Wu L, Gao F, Hong W, Jin G, Zhai Z. Size effects of vacancy formation and oxygen adsorption on gas-sensitive tin oxide semiconductor: a first principle study. Curr Nanosci. 2021;17(2):327–37. doi: 10.2174/1573413716999200817124021.
[31] Liu J, Bai Y, Shi J, Yu Q, Liu J, Yang J, et al. Selective detection of mercury ions based on tin oxide quantum dots: performance and fluorescence enhancement model. J Mater Chem C. 2021;9:8274–84. doi: 10.1039/D1TC00824B.
[32] Li J, Chen R, Cui W, Dong XA, Wang H, Kim KH, et al. Synergistic photocatalytic decomposition of a volatile organic compound mixture: High efficiency, reaction mechanism, and long-term stability. ACS Catal. 2020;10(13):7230–9. doi: 10.1021/acscatal.0c00693.
[33] Chen R, Li J, Sheng J, Cui W, Dong XA, Chen P, et al. Unveiling the unconventional roles of methyl number on the ring-opening barrier in photocatalytic decomposition of benzene, toluene and o-xylene. Appl Catal B. 2020;278:119318. doi: 10.1016/j.apcatb.2020.119318.
[34] Khan AF, Mehmood M, Aslam M, Ashraf M. Characteristics of electron beam evaporated nanocrystalline SnO_2 thin films annealed in air. Appl Surf Sci. 2010;256(7):2252–8. doi: 10.1016/j.apsusc.2009.10.047.
[35] Liu J, Zhang H, Li Y, Shen H, Ding Y, Su N, et al. Enhanced Vis-NIR light absorption and thickness effect of Mo-modified SnO_2 thin films: a first principle calculation study. Result Phys. 2021;23:103997. doi: 10.1016/j.rinp.2021.103997.
[36] Liu J, Xue W, Jin G, Zhai Z, Lv J, Hong W, et al. Preparation of tin oxide quantum dots in aqueous solution and applications in semiconductor gas sensors. Nanomaterials. 2019;9(2):240. doi: 10.3390/nano9020240.
[37] Liu J, Zhang Q, Xue W, Zhang H, Bai Y, Wu L, et al. Fluorescence characteristics of aqueous synthesized tin oxide quantum dots for the detection of heavy metal ions in contaminated water. Nanomaterials. 2019;9(9):1294. doi: 10.3390/nano9091294.
[38] Seki H, Ishisawa N, Mizutani N, Kato M. High temperature structures of the rutile-type oxides, TiO_2 and SnO_2. J Ceram Assoc Jpn. 1984;92:219–23. doi: 10.2109/jcersj1950.92.1064_219.
[39] Wang X, Di Q, Wang X, Zhao H, Liang B, Yang J. Effect of oxygen vacancies on photoluminescence and electrical properties of (200) oriented fluorine-doped SnO_2 films. Mater Sci Eng B Adv Funct Solid-State Mater. 2019;250:114433. doi: 10.1016/j.mseb.2019.114433.
[40] Liu J, Zhang Q, Tian X, Hong Y, Nie Y, Su N, et al. Highly efficient photocatalytic degradation of oil pollutants by oxygen deficient SnO_2 quantum dots for water remediation. Chem Eng J. 2021;404:127146. doi: 10.1016/j.cej.2020.127146.
[41] Tauc J, Grigorovici R, Vancu A. Optical properties and electronic structure of amorphous germanium. Phys Status Solidi (b). 1966;15(2):627–37. doi: 10.1002/pssb.19660150224.
[42] Liu J, Nie Y, Xue W, Wu L, Jin H, Jin G, et al. Size effects on structural and optical properties of tin oxide quantum dots with enhanced quantum confinement. J Mater Res Technol. 2020;9(4):8020–8. doi: 10.1016/j.jmrt.2020.05.041.
[43] Jarzebski ZM, Marton JP. Physical properties of SnO_2 materials: II. electrical properties. J Electrochem Soc. 1976;123(9):299C–310C. doi: 10.1149/1.2133090.
[44] Zhao Y, Zhang F, Zhang J, Zou K, Zhang J, Chen C, et al. Preparation of composite photocatalyst with tunable and self-indicating delayed onset of performance and its application in polyethylene degradation. Appl Catal B. 2021;286:119918. doi: 10.1016/j.apcatb.2021.119918.
[45] Ariza-Tarazona MC, Villarreal-Chiu JF, Hernández-López JM, Rivera De la Rosa J, Barbieri V, Siligardi C, et al. Microplastic pollution reduction by a carbon and nitrogen-doped TiO_2: effect of pH and temperature in the photocatalytic degradation process. J Hazard Mater. 2020;395:122632. doi: 10.1016/j.jhazmat.2020.122632.
[46] Venkataramana C, Botsa SM, Shyamala P, Muralikrishna R. Photocatalytic degradation of polyethylene plastics by $NiAl_2O_4$ spinels-synthesis and characterization. Chemosphere. 2021;265:129021. doi: 10.1016/j.chemosphere.2020.129021.
[47] Lam S-M, Sin J-C, Zeng H, Lin H, Li H, Chai Y-Y, et al. Green synthesis of Fe-ZnO nanoparticles with improved sunlight photocatalytic performance for polyethylene film deterioration and bacterial inactivation. Mater Sci Semicond Process. 2021;123:105574. doi: 10.1016/j.mssp.2020.105574.
[48] Ariza-Tarazona MC, Villarreal-Chiu JF, Barbieri V, Siligardi C, Cedillo-González EI. New strategy for microplastic degradation: Green photocatalysis using a protein-based porous N-TiO_2 semiconductor. Ceram Int. 2019;45(7):9618–24. doi: 10.1016/j.ceramint.2018.10.208.
[49] Olajire AA, Mohammed AA. Green synthesis of nickel oxide nanoparticles and studies of their photocatalytic activity in degradation of polyethylene films. Adv Powder Technol. 2020;31(1):211–8. doi: 10.1016/j.apt.2019.10.012.
[50] Li S, Xu S, He L, Xu F, Wang Y, Zhang L. Photocatalytic degradation of polyethylene plastic with polypyrrole/TiO_2 nanocomposite as photocatalyst. Polym Plast Technol Eng. 2010;49(4):400–6. doi: 10.1080/03602550903532166.
[51] Ali SS, Qazi IA, Arshad M, Khan Z, Voice TC, Mehmood CT. Photocatalytic degradation of low density polyethylene (LDPE) films using titania nanotubes. Environ Nanotechnol Monit Manag. 2016;5:44–53. doi: 10.1016/j.enmm.2016.01.001.
[52] Liang W, Luo Y, Song S, Dong X, Yu X. High photocatalytic degradation activity of polyethylene containing polyacrylamide grafted TiO_2. Polym Degrad Stab. 2013;98(9):1754–61. doi: 10.1016/j.polymdegradstab.2013.05.027.
[53] Sharma S, Basu S, Shetti NP, Nadagouda MN, Aminabhavi TM. Microplastics in the environment: occurrence, perils, and eradication. Chem Eng J. 2021;408:127317. doi: 10.1016/j.cej.2020.127317.